ACS MATERIALS Au
AN OPEN ACCESS JOURNAL OF THE AMERICAN CHEMICAL SOCIETY

pubs.acs.org/materialsau Article

Water-Responsive Self-Repairing Superomniphobic Surfaces via Regeneration of Hierarchical Topography

Mohammadamin Ezazi, Bishwash Shrestha, Anjana Maharjan, and Gibum Kwon*

Cite This: *ACS Mater. Au* 2022, 2, 55−62 Read Online

ACCESS | Metrics & More | Article Recommendations | Supporting Information

ABSTRACT: Superomniphobic surfaces that can self-repair physical damage are desirable for sustainable performance over time in many practical applications that include self-cleaning, corrosion resistance, and protective gears. However, fabricating such self-repairing superomniphobic surfaces has thus far been a challenge because it necessitates the regeneration of both low-surface-energy materials and hierarchical topography. Herein, a water-responsive self-repairing superomniphobic film is reported by utilizing cross-linked hydroxypropyl cellulose (HPC) composited with silica (SiO_2) nanoparticles (HPC-SiO_2) that is treated with a low-surface-energy perfluorosilane. The film can repair physical damage (e.g., a scratch) in approximately 10 s by regenerating its hierarchical topography and low-surface-energy material upon the application of water vapor. The repaired region shows an almost complete recovery of its inherent superomniphobic wettability and mechanical hardness. The repairing process is driven by the reversible hydrogen bond between the hydroxyl (−OH) groups which can be dissociated upon exposure to water vapor. This results in a viscous flow of the HPC-SiO_2 film into the damaged region. A mathematical model composed of viscosity and surface tension of the HPC-SiO_2 film can describe the experimentally measured viscous flow with reasonable accuracy. Finally, we demonstrate that the superomniphobic HPC-SiO_2 film can repair physical damage by a water droplet pinned on a damaged area or by sequential rolling water droplets.

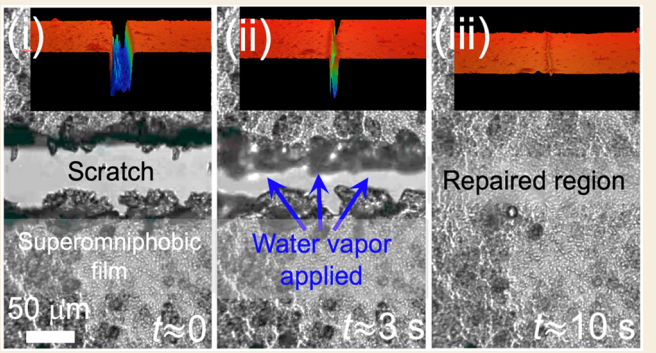

KEYWORDS: *superomniphobic surface, self-repairing, hydroxypropyl cellulose, dynamic hydrogen bonding, viscous flow*

INTRODUCTION

A surface that can repel liquids with both high (e.g., water) and low (e.g., oil) surface tension (γ_{lv}) has demonstrated potential for a wide range of practical applications including oil−water separation,[1−3] self-cleaning,[4,5] drag reduction,[6,7] and corrosion resistance[8,9] due to its extreme liquid repellency.[10] Designing such a superomniphobic surface [i.e., a surface that displays apparent contact angles (θ^*) greater than 150° and a roll-off angle (ω) less than 10° with virtually all liquids] involves a low-solid-surface-energy (γ_{sv}) coating along with surface roughness.[6] Unlike a superhydrophobic surface (i.e., a surface exhibiting $\theta^* > 150°$ and $\omega < 10°$ with water), we[6,8,11,12] and others[13,14] demonstrated that a superomniphobic surface must possess a re-entrant surface texture (i.e., convex or overhang topography[10]) which enables a composite solid−liquid−air interface even with a low-surface-tension liquid such as an oil. The composite interface can be further reinforced by a hierarchical surface topography (i.e., surface texture possessing two or more length scales[6]) which often involves a microscopic coarse texture along with finer-scale textures (i.e., typically nanometric scale).[15,16] However, such a re-entrant surface texture with a hierarchical topography often results in poor mechanical durability.[6] For example, a superomniphobic surface can be readily compromised because a low-surface-energy coating may become delaminated upon mechanical abrasion.[7,17] Also, the surface textures are delicate and tend to easily undergo physical damage.[17,18] Thus, developing mechanically durable superomniphobic surfaces has thus far been an active area of research.

A variety of strategies have been employed to enhance the mechanical durability of superomniphobic surfaces. For example, a low-surface-energy coating has been grafted or cross-linked directly to the substrate.[19,20] This strategy enhances mechanical durability[19] by eliminating the need for an intermediate binding layer which can easily be compromised upon external stresses. Also, inherently hard materials (e.g., ceramics[21,22] and metals[23,24]) have been employed in fabricating durable superomniphobic surfaces. Although these surfaces can maintain their extreme liquid repellency even after being subjected to mechanical stress, they are also vulnerable to

Received: August 10, 2021
Revised: September 13, 2021
Accepted: September 13, 2021
Published: October 13, 2021

https://doi.org/10.1021/acsmaterialsau.1c00036
ACS Mater. Au 2022, 2, 55−62

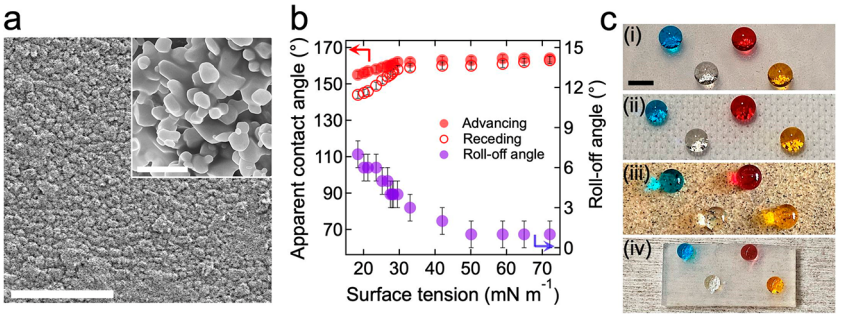

Figure 1. (a) SEM image showing the surface of an HPC-SiO_2 film that exhibits a hierarchical surface texture. The scale bar represents 20 μm. The inset demonstrates a high-magnification SEM image of nanoscale SiO_2 particles with re-entrant curvatures. The scale bar represents 1 μm. (b) Measured advancing and receding apparent contact angles, as well as roll-off angles for liquids with a broad range of surface tension values on an HPC-SiO_2 film. (c) Photographs of four droplets including ethanol (dyed blue, γ_{lv} = 22.1 mN m^{-1}), *n*-octane (dyed gray, γ_{lv} = 21.2 mN m^{-1}), *n*-heptane (dyed red, γ_{lv} = 20.1 mN m^{-1}), and *n*-hexane (dyed yellow, γ_{lv} = 18.4 mN m^{-1}) on an HPC-SiO_2 film fabricated on (i) stainless steel, (ii) polyester fabric, and (iii) ceramic-resin composite; (iv) freestanding HPC-SiO_2 film. The scale bar represents 3 mm.

physical damage upon cyclic loading or when being subjected to extremely high forces.[25]

In a new vein, superomniphobic surfaces that can repair physical damage and restore their inherent physicochemical properties have been reported.[2] Such self-repairing superomniphobic surfaces require restoring both surface chemistry (e.g., low-solid-surface-energy coating) and surface texture geometry (e.g., re-entrant and/or hierarchical surface texture).[26,27] Conventionally, these surfaces can initiate the repairing process in response to external triggers such as heat[8,28−30] and light irradiation.[31,32] For example, Zhou et al.[30] fabricated self-repairing superomniphobic coatings by using a mixture of low-surface-energy nanoparticles (e.g., polytetrafluoroethylene (PTFE) and DuPont Zonyl321) along with a fluorocarbon surfactant. The coating restored its superomniphobic wettability upon heating due to the migration of fluorinated alkyl chains toward the surface to lower the overall surface free energy. Zhao et al.[33] utilized a composite of epoxy resin and perfluorodecyl polysiloxane-modified silica nanoparticles to fabricate a self-healing superomniphobic coating on a metal substrate. The coating can recover its liquid repellency after repairing physical damage upon an increase in the temperature above its glass transition temperature (T_g). Dongli et al.[32] reported a self-healing superomniphobic coating prepared by using a combination of ultraviolet (UV) light-curable polyurethane acrylic resin and fluorinated alumina nanoparticles. The coating demonstrated an accelerated self-healing of physical damage under UV light irradiation. Recently, we[8] also reported a superomniphobic surface fabricated by reacting epoxidized soybean oil, perfluorinated epoxy, citric acid, and silica nanoparticles. The surface can repair a deep crack at a temperature above its glass transition temperature.

While heat or light has been extensively employed as a trigger to initiate the self-repairing process, the usage of water as a self-repairing trigger has been barely reported for these superrepellent surfaces despite its versatility and immediate availability in many practical applications. For example, Bai et al.[34] fabricated a superhydrophobic surface by sequentially spraying an epoxy resin and a mixture of poly(methyl methacrylate), zinc stearate, and stearic acid. The surface can repair damage when submerged in deionized (DI) water for 30 min and recover its original superhydrophobic wettability. Chen et al.[35] coated cotton fabric with layer-by-layer deposited branched poly(ethylenimine), ammonium polyphosphate, and fluorinated-decyl polyhedral oligomeric silsesquioxane. The coating can restore its compromised superhydrophobicity when exposed to an ambient environment with a relative humidity of 35% for 4 h after being subjected to oxygen (O_2) plasma or mechanical rubbing.

Fabricating a water-responsive superomniphobic surface that can repair physical damage requires the consideration of the following design criteria. First, the surface should acquire sufficient mobility when interacting with water to restore both a low-energy coating and rough texture. Also, the repairing process should be completed within a short period of time. This becomes critical when water is applied in its vapor form instead of as a liquid which can significantly retard the repairing process due to a limited number of available water molecules for interacting with the surface at a given condition (e.g., volume). Finally, the repaired region should exhibit its inherent mechanical and chemical properties. This may be particularly challenging for a surface that absorbs water molecules (e.g., hydrogel) because the abundant absorption of water often deteriorates the surface's physicochemical properties.

By considering these design criteria, herein, a water-responsive self-repairing superomniphobic film is developed by utilizing cross-linked hydroxypropyl cellulose (HPC) composited with SiO_2 nanoparticles that are treated with a low-surface-energy perfluorosilane. The film demonstrates that it can repair a deep scratch upon exposure to water vapor for ≈10 s and restore its inherent superomniphobic wettability and mechanical hardness. This can be attributed to the reversible hydrogen bonds between the free hydroxyl groups of the HPC-SiO_2 film which can be readily dissociated upon exposure to water vapor. Consequently, the HPC-SiO_2 film acquires sufficient mobility and demonstrates a viscous flow into a scratch resulting in repairing the damage. A mathematical model based on the glassy thin film equation is utilized to describe the viscous flow of the HPC-SiO_2 film. Finally, the film demonstrates that it can repair damage by a water droplet pinned on the damaged area or consecutive rolling water droplets at ambient conditions. We envision that our film can provide a viable solution for a protective coating against hostile environments in the marine, automotive, and aviation applications.

RESULTS AND DISCUSSION

We fabricated a self-repairing superomniphobic film by spraying a solution of HPC, glyoxal, and SiO_2 nanoparticles (average diameter ≈250 nm) with a weight ratio of 98:1:1 (HPC:glyox-

https://doi.org/10.1021/acsmaterialsau.1c00036
ACS Mater. Au 2022, 2, 55−62

al:SiO_2) on a glass substrate. Subsequent heat treatment at 50 °C for 15 min (Experimental Section) results in a cross-linked composite of HPC-SiO_2 due to the hydrolysis−condensation[36,37] of hydroxyl groups of HPC and SiO_2 with glyoxal (Supporting Information, Section 1). Note that glyoxal was used as a cross-linker while SiO_2 nanoparticles were used to create re-entrant surface texture.[8] The cross-linked HPC-SiO_2 film with a consolidated network enables the recovery of the original surface topography (i.e., re-entrant texture) when the HPC gains sufficient mobility upon exposure to water. To lower the overall solid surface energy, the HPC-SiO_2 film was vapor-deposited with 1*H*,1*H*,2*H*,2*H*-perfluorodecyltrichlorosilane (F-silane) at 130 °C for 60 min (Experimental Section). Note that hydrolysis of F-silane molecules results in silanol groups that can undergo polycondensation to form a covalent bond with any unreacted hydroxyl groups on the HPC-SiO_2 film.[38]

The resulting HPC-SiO_2 film exhibits a hierarchical texture with re-entrant curvatures composed of micro- and nanoscale SiO_2 aggregates (Figure 1a). The HPC-SiO_2 film exhibits very high contact angles for liquids with a broad range of surface tension (γ_{lv}) values (i.e., superomniphobic wettability) (Figure 1b and SI, Section 2). For example, the apparent advancing (θ^*_{adv}) and receding (θ^*_{rec}) contact angles of water (γ_{lv} = 72.1 mN m^{-1}) were measured as $\theta^*_{adv} = 164° \pm 3°$ and $\theta^*_{rec} = 163° \pm 2°$, respectively, while those for *n*-heptane (γ_{lv} = 20.1 mN m^{-1}) were measured as $\theta^*_{adv} = 156° \pm 3°$ and $\theta^*_{rec} = 145° \pm 3°$, at a relative humidity of ≈9% ± 3%. We also measured the apparent contact angles for water and *n*-heptane at a higher relative humidity (≈98%). Note that we acquired and maintained such a high relative humidity by water vapor with a flow rate of ≈0.5 mL min^{-1} at a distance of ≈30 cm in a custom-made humidifier (Experimental Section). The measured apparent contact angles for *n*-heptane were $\theta^*_{adv} = 155° \pm 2°$ and $\theta^*_{rec} = 143° \pm 2°$; those for water were $\theta^*_{adv} = 159° \pm 2°$ and $\theta^*_{rec} = 155° \pm 2°$. Such a slight decrease in the water apparent contact angles can be attributed to the condensation of water vapor on the surface which may partially replace the air pockets trapped between the solid and the contacting water droplet.[39]

We also measured the roll-off angles (i.e., minimum tilting angle, ω for a surface at which a contacting droplet starts to roll-off[40]) for these liquids. The results show that even a very low-surface-tension liquid such as *n*-heptane can exhibit a roll-off angle of $\omega = 6° \pm 1°$ on our HPC-SiO_2 film (see also Figure 1b). We also demonstrated that a droplet of *n*-dodecane (γ_{lv} = 25.3 mN m^{-1}, volume ≈ 5 μL) can bounce off our HPC-SiO_2 film two times before residing on the surface (Movie S1). Further, the contact angle for a droplet of ethanol:water mixture (80:20 vol:vol, γ_{lv} ≈ 24.3 mN m^{-1})[41] remained nearly unaffected while being evaporated, which corroborates that our HPC-SiO_2 film can form a robust solid−liquid−air composite interface (SI, Section 3). Please note that the measured apparent contact angles and the roll-off angles varied on the HPC-SiO_2 films prepared with varied spraying times (SI, Section 4).

The HPC-SiO_2 film can be readily fabricated on a variety of substrates including metal, fabric, composite, or even free-standing (Figure 1c). This is due to the dialdehyde chemistry of glyoxal that can strongly anchor to virtually any substrates via an acetalization reaction[42,43] which can form a covalent acetate linkage[44] with the underlying substrate (SI, Section 5).

Physical damage such as deep scratches, cracks, and cavities on a superomniphobic surface can irreversibly compromise its liquid repellency.[17,18] We demonstrated that our HPC-SiO_2 film can repair physical damage upon exposure to water vapor. First, a scratch (width ≈ 60.3 ± 2.1 μm) was engraved onto the HPC-SiO_2 film (thickness ≈ 100.1 ± 3.2 μm) by utilizing a razor blade. Please note that the scratch was engraved such that the underlying glass substrate was revealed (Figure 2ai). Upon exposure to water vapor with a flow rate of ≈0.5 mL min^{-1} at room temperature (≈22 °C), the scratch started to narrow down (Figure 2aii) and eventually disappeared at $t \approx 10$ s (Figure 2aiii). A movie showing the repairing of physical damage on our HPC-SiO_2 film upon the application of water vapor is provided in the Supporting Information (Movie S2).

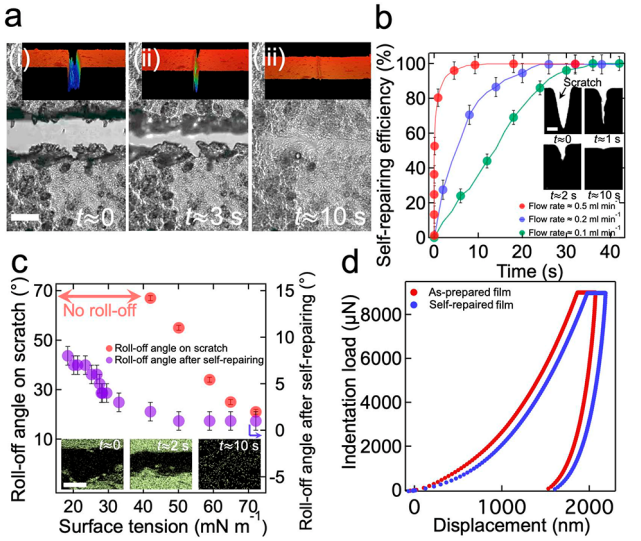

Figure 2. (a) Time-sequence optical microscopy images showing self-repairing of a scratch on the HPC-SiO_2 film upon introducing water vapor (flow rate ≈ 0.5 mL min^{-1}). The scale bar represents 50 μm. The inset shows cross-sectional optical profilometry images of a scratch during the repairing process. (b) Time-dependent plots of self-repairing efficiency (ζ) at different flow rates of water vapor. The inset shows time-dependent cross-section photographs of a scratch (width ≈ 59 μm and depth ≈ 100 μm) engraved on the HPC-SiO_2 film undergoing a repairing process when exposed to water vapor with a flow rate of ≈0.5 mL min^{-1}. The scale bar is 50 μm. (c) Measured roll-off angles (ω) for liquids with a broad range of surface tension values placed on a repaired region. For a comparison, the ω values on the scratch are also provided. The inset shows time-sequence energy dispersive X-ray spectroscopy (EDS) maps for fluorine on a scratch. The scale bar is 50 μm. (d) Plot of the measured load−displacement on the repaired region on the HPC-SiO_2 film. For a comparison, the plot for the as-prepared surface is also shown.

Figure 2b shows the plots of self-repairing efficiency as a function of exposure time at different flow rates of water vapor. The values of ζ start to rapidly increase upon exposure to water vapor with a flow rate of ≈0.5 mL min^{-1} and reach $\zeta \approx 100\%$ at $t \approx 10$ s, which indicates that a scratch disappeared completely. When the water vapor was introduced at a lower flow rate of ≈0.1 or ≈0.2 mL min^{-1}, complete reparation ($\zeta \approx 100\%$) was observed at $t \approx 36$ s and $t \approx 24$ s, respectively. We showed that a scratch on our HPC-SiO_2 film can be repaired by ethanol vapor (SI, Section 7).

https://doi.org/10.1021/acsmaterialsau.1c00036
ACS Mater. Au 2022, 2, 55−62

To demonstrate that our HPC-SiO_2 film can recover its inherent superomniphobic wettability, we measured the roll-off angles for liquids after the scratch was repaired. A liquid droplet was placed on a region where the scratch was engraved and repaired. By comparing the ω values with those measured on the as-prepared surface, we verified that our HPC-SiO_2 film exhibited a nearly complete recovery of its inherent superomniphobic wettability (Figure 2c). This is a result of restoring both its hierarchical surface texture and low-solid-surface-energy coating in the damaged region (see also the inset images in Figure 2c). We also demonstrated that our HPC-SiO_2 film can restore its superomniphobic wettability after repeated damage−repairing cycles (SI, Section 8).

We conducted the nanoindentation test[45] on the repaired region of the HPC-SiO_2 film (Experimental Section). The results show that the maximum indentation load (F = 9000 μN) resulted in a displacement (h) value of h = 2185 nm on the repaired region which is close to that measured on the as-prepared film (h = 2070 nm) (Figure 2d). This clearly indicates that our HPC-SiO_2 film can recover its inherent mechanical hardness after repairing physical damage.

Our HPC-SiO_2 film's ability to repair damage and recover its mechanical hardness can be attributed to the reversible hydrogen bonds between the hydroxyl groups in the HPC which can be dissociated upon exposure to water molecules.[46] This enables an HPC-SiO_2 film to exhibit a viscous flow into the scratch cavity and repair it (Scheme 1). Subsequently, the

Scheme 1. Illustration of the Proposed Self-Repairing Process of HPC-SiO_2 Film upon Water Vapor Exposure by Reversible Hydrogen Bonds between Free Hydroxyl Groups

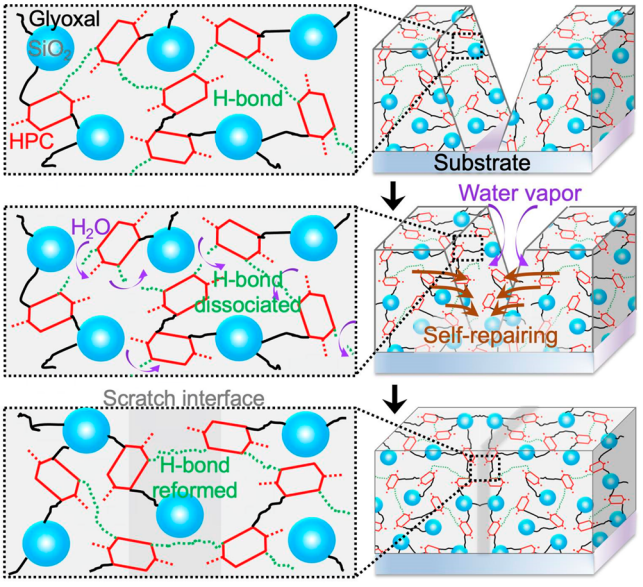

dissociated hydrogen bonds can be reformed in the absence of water vapor which enables the HPC-SiO_2 film to demonstrate repeated damage−repairing cycles. Please note that the absorption of water by the HPC-SiO_2 film is negligible (SI, Section 9).

By assuming that the reversible hydrogen bond is a driving force for the repairing process, a cross-linker (i.e., glyoxal) concentration can directly affect the extent of repair. To prove this, we conducted damage−repairing experiments on the HPC-SiO_2 films cross-linked with various glyoxal concentrations (e.g., 1.0%, 5.0%, and 10.0% of glyoxal with respect to HPC weight). Please note that the SiO_2 concentration remains the same (i.e., 1.0%) with respect to HPC and glyoxal weight. The HPC-SiO_2 films (thickness ≈ 100 μm) were engraved with a deep scratch (width ≈ 60.5 ± 1.7 μm and depth ≈ 100.2 ± 2.1 μm) followed by exposure to water vapor with a flow rate of ≈0.5 mL min^{-1}. Figure 3a shows the measured self-repairing efficiency values (ζ)

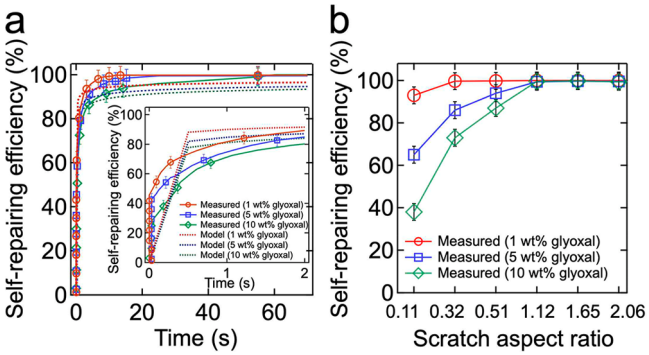

Figure 3. (a) Measured time-dependent self-repairing efficiency (ζ) values on the HPC-SiO_2 films prepared with varying glyoxal concentrations upon exposure to water vapor (flow rate ≈ 0.5 mL min^{-1}). The calculated ζ_{model} values by using eq 1 match reasonably well with the experimental data. The inset shows a zoomed-in plot during the first 2 s. (b) Plot of the measured highest ζ values on the HPC-SiO_2 films prepared with varying glyoxal concentrations engraved with scratches of different aspect ratios (α). Water vapor was applied with a constant flow rate of ≈0.5 mL min^{-1} until either the width or the depth of a scratch remains unchanged.

as a function of water vapor exposure time (Experimental Section). The results show that the HPC-SiO_2 film cross-linked with a 1.0 wt % glyoxal reached $\zeta \approx 100\%$ at $t \approx 10$ s whereas that prepared with 10.0 wt % glyoxal exhibited $\zeta \approx 100\%$ at $t \approx 60$ s. A more rapid repairing process on a film cross-linked with a lower glyoxal concentration is a consequence of a reduced structural restraint and a larger free volume between the HPC chains which facilitates the penetration of water molecules.[46] This results in an accelerated increase in the chain mobility of HPC upon exposure to water vapor.

The time-dependent evolution of a vertical profile ($H(x, t)$) of a scratch can be described by the glassy thin film equation[47,48] which is given as

$$\partial H(x, t)/\partial t + \gamma H_m^3/3\eta \times \partial^4 H(x, t)/\partial x^4 = 0 \quad (1)$$

where H_m, η (Pa s), and γ (mN m^{-1}) are the height (i.e., thickness), viscosity, and surface tension of the HPC-SiO_2 film, respectively. It has been demonstrated[47] that physical damage engraved on a film of glassy polymer (i.e., amorphous polymers that can demonstrate a glass transition temperature[49]) can exhibit time-dependent evolution in its vertical profile ($H(x, t)$) when it gains mobility. Please note that HPC has a high degree of amorphous content[50] and shows a glass transition temperature (SI, Section 10).[51] By assuming $H(x, t)$ as an infinitesimal step function and by utilizing a Fourier transform,[52] eq 1 can be solved for ($H(x, t)$). Please note that the values of η and γ utilized in the equation are experimentally determined (SI, Section 11). The calculated values of $H(x, t)$ were then utilized to determine the theoretical self-repairing efficiency according to the relation $\zeta_{model} = (H(x, t)/H_m) \times 100$. The results show that the calculated values of ζ_{model} by using eq 1 and the experimentally measured ζ values match reasonably well (see

https://doi.org/10.1021/acsmaterialsau.1c00036
ACS Mater. Au 2022, 2, 55−62

Figure 3a). Please note that the values of η and γ of our HPC-SiO_2 film showed insignificant change upon varied water vapor exposure time (SI, Section 12) which can be attributed to a combinatorial effect of negligible absorption and rapid evaporation of water vapor by the HPC-SiO_2 film (see also Section 9 in the SI). Further, we demonstrated that the adhesion strength of the HPC-SiO_2 film to the underlying substrate was not significantly affected after being exposed to water vapor (SI, Section 13).

Based on eq 1, it can be inferred that the viscous flow-driven reparation on our HPC-SiO_2 film can be limited when the width or depth of a scratch is too wide or deep. For example, when a scratch is too wide, the two edges of the HPC-SiO_2 film may not meet each other, which can result in incomplete repairing. To study our HPC-SiO_2 film's repairing capability, we prepared HPC-SiO_2 films with varying glyoxal concentrations and engraved a scratch with different ratios of the depth to the width (i.e., aspect ratio, $\alpha \approx 0.11$, 0.32, 0.51, 1.12, 1.65, and 2.06). Please note that the thickness (i.e., depth of scratch) of all HPC-SiO_2 films was approximately 100 μm. All films were subjected to water vapor with a flow rate of ≈0.5 mL min^{-1} until either the width or the depth of a scratch remained unchanged. Subsequently, we calculated the self-repairing efficiency values based on the cross-sectional area of the scratches (see also Section 6 in the SI). Figure 3b shows the values of ζ as a function of α values. The results show that all HPC-SiO_2 films exhibited $\zeta \approx 100\%$ when $\alpha \geq 1.12$ (i.e., $\alpha = 1.12$, 1.65, and 2.06) while they demonstrated incomplete repairing when $\alpha \leq 0.51$ (i.e., $\alpha =$ 0.51, 0.32, and 0.11). For example, when $\alpha = 0.11$ (i.e., depth ≈ 100 μm and width ≈ 908 μm), the self-repairing efficiency values were measured as ≈93%, ≈65%, and ≈38%, respectively, for HPC-SiO_2 films prepared with glyoxal concentrations of 1.0, 5.0, and 10.0 wt %. Despite the fact that a scratch can be partially repaired when $\alpha \leq 0.51$, a liquid droplet can still maintain the Cassie−Baxter state[53] if it forms a robust composite solid−air−liquid interface. For example, when a liquid droplet touches the underlying substrate (e.g., a clean glass slide), it may transition to the "fully wetted" Wenzel state[54] which often results in a loss of super-repellency. On the other hand, when the two edges of the dissected film come close enough, our film can exhibit its inherent superomniphobic wettability although self-repairing efficiency is not 100%. This is possible because our HPC-SiO_2 film possesses a monolithic configuration which enables the edges to show the same surface chemistry and topography as those of the topmost surface.

We demonstrated that our HPC-SiO_2 film can recover its superomniphobic wettability even for a pinned water droplet placed on a deep scratch (Figure 4a). As a water droplet (volume = 5 μL) gradually evaporates in ambient conditions (i.e., temperature ≈ 22 °C and relative humidity ≈ 9% ± 3%), the scratch (≈101.4 ± 1.9 μm deep and ≈60.3 ± 2.5 μm wide) becomes narrower. Eventually, a water droplet abruptly departs and rolls off the surface at $t \approx 56$ s (Figure 4b). Note that a water droplet remained pinned without spreading on the HPC-SiO_2 film tilted at an angle of ≈10° relative to the horizontal plane. A movie illustrating the in situ recovery of super-repellency of our HPC-SiO_2 surface by a stationary water droplet is included as Movie S3.

Finally, we demonstrated that consecutive rolling water droplets can repair a deep scratch on our HPC-SiO_2 film[55] (Figure 4c). The water droplets with a constant volume (5 μL) were consecutively introduced to the top of the film by using a syringe pump with a constant interdroplet time interval of ≈0.5 s

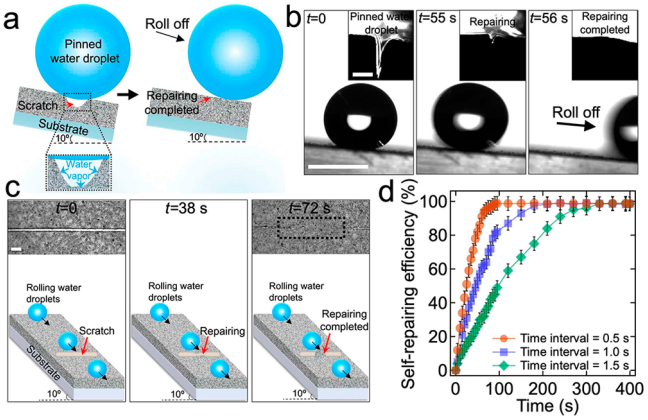

Figure 4. Schematic (a) and time-sequence snapshots (b) illustrating a pinned water droplet that repairs a scratch on an HPC-SiO_2 film and subsequently departs and rolls off after the completion of the reparation. The scale bar in part b represents 2 mm. The inset shows cross-sectional images of a scratch undergoing self-repairing by a pinned water droplet. The scale bar in the inset is 100 μm. (c) Schematic illustrating the self-repairing of a scratch on an HPC-SiO_2 film by sequential rolling water droplets. The inset shows optical microscopy images of a scratch region in contact with rolling water droplets. The scale bar in the inset is 150 μm. (d) Measured self-repairing efficiency of a scratch on an HPC-SiO_2 film by sequential rolling water droplets dispensed at varied time intervals (0.5, 1.0, and 1.5 s).

(Experimental Section). The film was tilted to 10° with respect to the horizontal plane such that rolling water droplets are not pinned on the scratch (≈100.6 ± 2.0 μm deep and ≈60.1 ± 2.6 μm wide). We measured the contact time of each rolling water droplet with the scratch region as ≈0.1 s by using a high-speed camera image analysis. An optical microscopy image confirms that the region of a scratch subjected to rolling water droplets disappeared at $t \approx 72$ s (see the inset in Figure 4c). We varied the interdroplet interval time and measured the self-repairing efficiency (Figure 4d).[55] The water droplets introduced at a shorter interdroplet interval can result in a more rapid reparation. A movie illustrating the self-repairing of a scratch by consecutive rolling water droplets on our HPC-SiO_2 film is included as Movie S4. Self-repairing by consecutive rolling water droplets is highly desirable in real-world applications. For example, when a vehicle is coated with a water-responsive self-repairing coating with super-repellency, physical damage can be readily repaired by rain droplets.

Despite promising results, the reliance on environmental conditions is a shortcoming of our water-responsive self-repairing HPC-SiO_2 film. For example, when the film is subjected to an extremely cold environment, the applied water vapor can be deposited as ice or frost on the surface. As a consequence, the water molecules cannot be readily accessible to the HPC-SiO_2 film, which can retard the self-repairing process.

CONCLUSIONS

We have developed a water-responsive self-repairing superomniphobic film by utilizing a cross-linked HPC-SiO_2 composite treated with a low-surface-energy perfluorosilane. The HPC-SiO_2 film can repair a deep scratch and restore its inherent superomniphobic wettability and mechanical hardness upon exposure to water vapor. Our film's self-repairing capability can be attributed to the reversible hydrogen bonds

https://doi.org/10.1021/acsmaterialsau.1c00036
ACS Mater. Au 2022, 2, 55−62

between the hydroxyl groups in the HPC-SiO_2 film which can be dissociated upon exposure to water molecules. Consequently, the HPC-SiO_2 film acquires sufficient mobility and demonstrates a viscous flow into a scratch cavity resulting in repairing the damage. We demonstrated that a mathematical model based on the glassy thin film equation can describe the experimentally measured time-dependent evolution of a scratch profile with reasonable accuracy. We also showed that a water droplet pinned on a scratch can depart and roll off the surface after repairing it. Finally, we demonstrated that consecutive rolling water droplets can repair a deep scratch engraved on our superomniphobic HPC-SiO_2 film. We envision that our water-responsive self-repairing superomniphobic surface can offer extensive utility in the marine, automotive, and aviation industries.

EXPERIMENTAL SECTION

Fabrication of an HPC-SiO_2 Self-Repairing Superomniphobic Film

A solution of HPC, glyoxal, and SiO_2 nanoparticles (average diameter ≈ 250 nm) was prepared in deionized (DI) water. The overall concentration of the solute was 25.0 wt %. The weight ratio of HPC, glyoxal, and SiO_2 was 98:1:1. The solution was then sprayed (iWata spray gun) onto a variety of substrates including a glass slide, ceramic-resin composite, and polyester fabric (Anticon Sterile 100) followed by heat treatment at 50 °C for 15 min in a vacuum oven. Note that the spraying air pressure and the distance between the spraying gun and the substrate were maintained at 20 psi and 10 cm, respectively. Finally, the HPC-SiO_2 film was treated by chemical vapor deposition of 1*H*,1*H*,2*H*,2*H*-perfluorodecyltrichlorosilane (F-silane) at 130 °C for 60 min. A freestanding HPC-SiO_2 film was fabricated by spraying the solution on a glass slide which was pretreated with F-silane. After heat treatment at 50 °C for 60 min, the resulting HPC-SiO_2 film was carefully detached from the glass slide and subjected to F-silane treatment. Note that all HPC-SiO_2 films were thoroughly rinsed with excessive ethanol after fabrication.

Self-Repairing Tests

Self-repairing tests were conducted by utilizing a custom-made humidifier that is equipped with a water container (volume = 200 mL) and a nozzle (length = 10 cm) that can guide the generated water vapor to the area of interest in the HPC-SiO_2 films. The distance between the nozzle tip and the surface was maintained at 5 cm, and the flow rate of water vapor was maintained at ≈0.5 mL min^{-1}. Note that the relative humidity of the surrounding environment was maintained very low (i.e., relative humidity ≈9% ± 3%) to minimize the contribution to the self-repairing process by environment humidity.

Contact Angle Measurement

All contact angles were measured by advancing or receding ≈5 μL of liquids onto the surface utilizing a ramé-hart 190-U1 goniometer.

Scanning Electron Microscopy

The surface morphology of the HPC-SiO_2 films was investigated by utilizing field emission scanning electron microscopy (FE-SEM, FEI Versa 3D DualBeam) at an accelerating voltage of 5.0 kV. All films were sputter coated with a thin layer of gold (≈5 nm) to prevent charging.

Optical Profilometry

The arithmetic mean surface roughness (R_a) was measured by utilizing an optical profiler (Veeco Wyko NT 1100) at a scan rate of 50 nm s^{-1}. The optical profiler was also utilized for measuring the time-dependent evolution of a scratch profile during the repairing process while being continuously exposed to water vapor.

Nanoindentation

By utilizing nanoindentation (Hysitron TS 75 Triboscope), the loading−unloading was performed at a constant rate of 10.0 mN min^{-1}. The maximum indentation load and the holding time at the maximum load were set to 9000 μN and 3.0 s, respectively.

Measuring the Viscosity of the HPC-SiO_2 Film

The viscosity (η) values of the HPC-SiO_2 films prepared with varied glyoxal concentrations were measured by using a viscometer (Anton Paar MCR 302). The viscometer was operated in an amplitude sweep mode while keeping the oscillation frequency at a constant value of 1.0 Hz. Note that the measurements were conducted at room temperature (≈22 °C)

Self-Repairing Tests by Rolling Water Droplets

The self-repairing test by consecutive rolling water droplets was performed by utilizing a syringe pump (KD Scientific) dispensing water droplets (≈5 μL) at varied interdroplet time intervals of 0.5, 1.0, and 1.5 s. A high-speed camera (FASTEC IL5) equipped with high-magnification optics (Navitar Resolv4K and Mitutoyo 10× objective) was operated at 900 frames per second to measure the contact time of each rolling water droplet on the scratch region.

ASSOCIATED CONTENT

Supporting Information

The Supporting Information is available free of charge at https://pubs.acs.org/doi/10.1021/acsmaterialsau.1c00036.

Additional data and figures including a schematic, Fourier-transform infrared (FT-IR) spectroscopy analysis, liquid wettability, evaporation of an ethanol−water droplet, effect of spraying time on the liquid wettability, fabricating HPC-SiO_2 films on various substrates, calculating the cross-sectional area of a scratch, self-repairing by vapor of ethanol, recovery of superomniphobic wettability after multiple damage-repairing cycles, water vapor absorption, characterizing the glass transition temperature, dynamic viscosity, and surface tension values, effect of water vapor exposure time on dynamic viscosity and surface tension values, and adhesion strength (PDF)

Movie S1: a droplet of *n*-dodecane can bounce off an HPC-SiO_2 film (MP4)

Movie S2: self-repairing of a deep scratch on an HPC-SiO_2 film upon exposure to water vapor (MP4)

Movie S3: an HPC-SiO_2 film can recover its extreme liquid repellency for a pinned water droplet placed on a deep scratch after repairing it (MP4)

Movie S4: self-repairing of a deep scratch on an HPC-SiO_2 film by consecutive rolling water droplets (MP4)

AUTHOR INFORMATION

Corresponding Author

Gibum Kwon − *Department of Mechanical Engineering, University of Kansas, Lawrence, Kansas 66045, United States;* orcid.org/0000-0002-7192-1910; Email: gbkwon@ku.edu

Authors

Mohammadamin Ezazi − *Department of Mechanical Engineering, University of Kansas, Lawrence, Kansas 66045, United States;* orcid.org/0000-0003-2284-9809

Bishwash Shrestha − *Department of Mechanical Engineering, University of Kansas, Lawrence, Kansas 66045, United States;* orcid.org/0000-0003-0045-8890

Anjana Maharjan − *Department of Mechanical Engineering, University of Kansas, Lawrence, Kansas 66045, United States*

Complete contact information is available at:

https://doi.org/10.1021/acsmaterialsau.1c00036
ACS Mater. Au 2022, 2, 55−62

https://pubs.acs.org/10.1021/acsmaterialsau.1c00036

Author Contributions

M.E., B.S., and A.M. performed the experiments, analyzed data, and wrote the manuscript. G.K. conceived the project, designed the experiments, and wrote the manuscript.

Notes

The authors declare no competing financial interest.

■ ACKNOWLEDGMENTS

This research was supported by National Science Foundation [Award CBET-1944314], NASA Kansas EPSCoR [Award R52123-20-02314], and Kansas Corn Commission [Award 1000350]. We thank Dr. D. Ahn at the University of Texas, Dr. S. Seo at the Pusan National University, and Dr. J. Kang at the University of Illinois for the use of facilities.

■ REFERENCES

(1) Wang, Y.; Liu, Y.; Li, J.; Chen, L.; Huang, S.; Tian, X. Fast Self-Healing Superhydrophobic Surfaces Enabled by Biomimetic Wax Regeneration. *Chem. Eng. J.* **2020**, *390*, 124311.
(2) Zhou, H.; Wang, H.; Niu, H.; Lin, T. Recent Progress in Durable and Self-Healing Super-Nonwettable Fabrics. *Adv. Mater. Interfaces* **2018**, *5* (16), 1800461.
(3) Tian, X.; Jokinen, V.; Li, J.; Sainio, J.; Ras, R. H. A. Unusual Dual Superlyophobic Surfaces in Oil−Water Systems: The Design Principles. *Adv. Mater.* **2016**, *28* (48), 10652−10658.
(4) Kang, S. M.; Choi, J. S.; An, J. H. Reliable and Robust Fabrication Rules for Springtail-Inspired Superomniphobic Surfaces. *ACS Appl. Mater. Interfaces* **2020**, *12* (18), 21120−21126.
(5) Wang, W.; Liu, R.; Chi, H.; Zhang, T.; Xu, Z.; Zhao, Y. Durable Superamphiphobic and Photocatalytic Fabrics: Tackling the Loss of Super-Non-Wettability Due to Surface Organic Contamination. *ACS Appl. Mater. Interfaces* **2019**, *11* (38), 35327−35332.
(6) Kota, A. K.; Kwon, G.; Tuteja, A. The Design and Applications of Superomniphobic Surfaces. *NPG Asia Mater.* **2014**, *6* (7), e109.
(7) Kota, A. K.; Choi, W.; Tuteja, A. Superomniphobic Surfaces: Design and Durability. *MRS Bull.* **2013**, *38* (5), 383−390.
(8) Ezazi, M.; Shrestha, B.; Klein, N.; Lee, D. H.; Seo, S.; Kwon, G. Self-Healable Superomniphobic Surfaces for Corrosion Protection. *ACS Appl. Mater. Interfaces* **2019**, *11* (33), 30240−30246.
(9) Pan, S.; Kota, A. K.; Mabry, J. M.; Tuteja, A. Superomniphobic Surfaces for Effective Chemical Shielding. *J. Am. Chem. Soc.* **2013**, *135* (2), 578−581.
(10) Wang, W.; Salazar, J.; Vahabi, H.; Joshi-Imre, A.; Voit, W. E.; Kota, A. K. Metamorphic Superomniphobic Surfaces. *Adv. Mater.* **2017**, *29* (27), 1700295.
(11) Kota, A. K.; Kwon, G.; Choi, W.; Mabry, J. M.; Tuteja, A. Hygro-Responsive Membranes for Effective Oil−Water Separation. *Nat. Commun.* **2012**, *3*, 1025.
(12) Kwon, G.; Kota, A. K.; Li, Y.; Sohani, A.; Mabry, J. M.; Tuteja, A. On-Demand Separation of Oil-Water Mixtures. *Adv. Mater.* **2012**, *24* (27), 3666−3671.
(13) Panter, J.; Gizaw, Y.; Kusumaatmaja, H. Multifaceted Design Optimization for Superomniphobic Surfaces. *Sci. Adv.* **2019**, *5* (6), eaav7328.
(14) Liu, T.; Kim, C.-J. Turning a Surface Superrepellent Even to Completely Wetting Liquids. *Science* **2014**, *346* (6213), 1096−1100.
(15) Lee, S.; Kim, W.; Yim, C.; Yong, K.; Jeon, S. Growth of Hierarchical Gold Clusters for Use in Superomniphobic Electrodes. *RSC Adv.* **2019**, *9* (2), 761−765.
(16) Jang, H.; Lee, H. S.; Lee, K.-S.; Kim, D. R. Facile Fabrication of Superomniphobic Polymer Hierarchical Structures for Directional Droplet Movement. *ACS Appl. Mater. Interfaces* **2017**, *9* (11), 9213−9220.
(17) Milionis, A.; Loth, E.; Bayer, I. S. Recent Advances in the Mechanical Durability of Superhydrophobic Materials. *Adv. Colloid Interface Sci.* **2016**, *229*, 57−79.
(18) Tian, X.; Verho, T.; Ras, R. H. Moving Superhydrophobic Surfaces toward Real-World Applications. *Science* **2016**, *352* (6282), 142−143.
(19) Li, F.; Du, M.; Zheng, Q. Dopamine/Silica Nanoparticle Assembled, Microscale Porous Structure for Versatile Superamphiphobic Coating. *ACS Nano* **2016**, *10* (2), 2910−2921.
(20) Liu, S.; Zhou, H.; Wang, H.; Yang, W.; Shao, H.; Fu, S.; Zhao, Y.; Liu, D.; Feng, Z.; Lin, T. Argon-Plasma Reinforced Superamphiphobic Fabrics. *Small* **2017**, *13* (40), 1701891.
(21) Wang, D.; Sun, Q.; Hokkanen, M. J.; Zhang, C.; Lin, F.-Y.; Liu, Q.; Zhu, S.-P.; Zhou, T.; Chang, Q.; He, B. Design of Robust Superhydrophobic Surfaces. *Nature* **2020**, *582* (7810), 55−59.
(22) Li, S.-Y.; Wang, J.; Li, Y.; Wang, C.-W. Superhydrophobic Surface Based on Self-Aggregated Alumina Nanowire Clusters Fabricated by Anodization. *Microelectron. Eng.* **2015**, *142*, 70−76.
(23) Barthwal, S.; Kim, Y. S.; Lim, S.-H. Mechanically Robust Superamphiphobic Aluminum Surface with Nanopore-Embedded Microtexture. *Langmuir* **2013**, *29* (38), 11966−11974.
(24) Wang, H.; He, M.; Liu, H.; Guan, Y. One-Step Fabrication of Robust Superhydrophobic Steel Surfaces with Mechanical Durability, Thermal Stability, and Anti-Icing Function. *ACS Appl. Mater. Interfaces* **2019**, *11* (28), 25586−25594.
(25) Esteves, A.; Luo, Y.; Van de Put, M.; Carcouët, C.; De With, G. Self-Replenishing Dual Structured Superhydrophobic Coatings Prepared by Drop-Casting of an All-in-One Dispersion. *Adv. Funct. Mater.* **2014**, *24* (7), 986−992.
(26) Wang, H.; Zhou, H.; Gestos, A.; Fang, J.; Lin, T. Robust, Superamphiphobic Fabric with Multiple Self-Healing Ability against Both Physical and Chemical Damages. *ACS Appl. Mater. Interfaces* **2013**, *5* (20), 10221−10226.
(27) Li, B.; Zhang, J. Durable and Self-Healing Superamphiphobic Coatings Repellent Even to Hot Liquids. *Chem. Commun.* **2016**, *52* (13), 2744−2747.
(28) Zhang, H.; Liu, Y.; Hou, C.; Ma, Y.; Zhang, B.; Zhang, H.; Zhang, Q. Low-Maintenance Superamphiphobic Coating Based on a Smart Two-Layer Self-Healing Network. *Surf. Coat. Technol.* **2017**, *331*, 97−106.
(29) Zhang, H.; Tan, J.; Liu, Y.; Hou, C.; Ma, Y.; Gu, J.; Zhang, B.; Zhang, H.; Zhang, Q. Design and Fabrication of Robust, Rapid Self-Healable, Superamphiphobic Coatings by a Liquid-Repellent "Glue+Particles" Approach. *Mater. Des.* **2017**, *135*, 16−25.
(30) Zhou, H.; Wang, H.; Niu, H.; Zhao, Y.; Xu, Z.; Lin, T. A Waterborne Coating System for Preparing Robust, Self-Healing, Superamphiphobic Surfaces. *Adv. Funct. Mater.* **2017**, *27* (14), 1604261.
(31) Shang, B.; Chen, M.; Wu, L. Fabrication of Uv-Triggered Liquid-Repellent Coatings with Long-Term Self-Repairing Performance. *ACS Appl. Mater. Interfaces* **2018**, *10* (37), 31777−31783.
(32) Zhao, D.; Du, Z.; Liu, S.; Wu, Y.; Guan, T.; Sun, Q.; Sun, N.; Ren, B. Uv Light Curable Self-Healing Superamphiphobic Coatings by Photopromoted Disulfide Exchange Reaction. *ACS Appl. Polym. Mater.* **2019**, *1* (11), 2951−2960.
(33) Zhao, X.; Wei, J.; Li, B.; Li, S.; Tian, N.; Jing, L.; Zhang, J. A Self-Healing Superamphiphobic Coating for Efficient Corrosion Protection of Magnesium Alloy. *J. Colloid Interface Sci.* **2020**, *575*, 140−149.
(34) Bai, N.; Li, Q.; Dong, H.; Tan, C.; Cai, P.; Xu, L. A Versatile Approach for Preparing Self-Recovering Superhydrophobic Coatings. *Chem. Eng. J.* **2016**, *293*, 75−81.
(35) Chen, S.; Li, X.; Li, Y.; Sun, J. Intumescent Flame-Retardant and Self-Healing Superhydrophobic Coatings on Cotton Fabric. *ACS Nano* **2015**, *9* (4), 4070−4076.
(36) Mahmoud, M. E.; Abdou, A. E.; Sobhy, M. E. Engineered Nano-Zirconium Oxide-Crosslinked-Nanolayer of Carboxymethyl Cellulose for Speciation and Adsorptive Removal of Cr (Iii) and Cr (Vi). *Powder Technol.* **2017**, *321*, 444−453.

(37) Kim, G.-H.; Ramesh, S.; Kim, J.-H.; Jung, D.; Kim, H. S. Cellulose-Silica/Gold Nanomaterials for Electronic Applications. *J. Nanosci. Nanotechnol.* **2014**, *14* (10), 7495−7501.
(38) Akram Raza, M.; Kooij, E. S.; van Silfhout, A.; Poelsema, B. Superhydrophobic Surfaces by Anomalous Fluoroalkylsilane Self-Assembly on Silica Nanosphere Arrays. *Langmuir* **2010**, *26* (15), 12962−12972.
(39) Han Yeong, Y.; Steele, A.; Loth, E.; Bayer, I.; De Combarieu, G.; Lakeman, C. Temperature and Humidity Effects on Superhydrophobicity of Nanocomposite Coatings. *Appl. Phys. Lett.* **2012**, *100* (5), No. 053112.
(40) Qahtan, T. F.; Gondal, M. A.; Dastageer, M. A.; Kwon, G.; Ezazi, M.; Al-Kuban, M. Z. Thermally Sensitized Membranes for Crude Oil−Water Remediation under Visible Light. *ACS Appl. Mater. Interfaces* **2020**, *12* (43), 48572−48579.
(41) Vazquez, G.; Alvarez, E.; Navaza, J. M. Surface Tension of Alcohol Water+ Water from 20 to 50. Degree. C. *J. Chem. Eng. Data* **1995**, *40* (3), 611−614.
(42) Choi, H. M.; Kim, J. H.; Shin, S. Characterization of Cotton Fabrics Treated with Glyoxal and Glutaraldehyde. *J. Appl. Polym. Sci.* **1999**, *73* (13), 2691−2699.
(43) Yang, Q.; Dou, F.; Liang, B.; Shen, Q. Studies of Cross-Linking Reaction on Chitosan Fiber with Glyoxal. *Carbohydr. Polym.* **2005**, *59* (2), 205−210.
(44) Zhu, H.; Narakathu, B. B.; Fang, Z.; Aijazi, A. T.; Joyce, M.; Atashbar, M.; Hu, L. A Gravure Printed Antenna on Shape-Stable Transparent Nanopaper. *Nanoscale* **2014**, *6* (15), 9110−9115.
(45) Oliver, W. C.; Pharr, G. M. An Improved Technique for Determining Hardness and Elastic Modulus Using Load and Displacement Sensing Indentation Experiments. *J. Mater. Res.* **1992**, *7* (6), 1564−1583.
(46) Spoljaric, S.; Salminen, A.; Luong, N. D.; Seppälä, J. Stable, Self-Healing Hydrogels from Nanofibrillated Cellulose, Poly (Vinyl Alcohol) and Borax Via Reversible Crosslinking. *Eur. Polym. J.* **2014**, *56*, 105−117.
(47) Chai, Y.; Salez, T.; McGraw, J. D.; Benzaquen, M.; Dalnoki-Veress, K.; Raphaël, E.; Forrest, J. A. A Direct Quantitative Measure of Surface Mobility in a Glassy Polymer. *Science* **2014**, *343* (6174), 994−999.
(48) Salez, T.; McGraw, J. D.; Bäumchen, O.; Dalnoki-Veress, K.; Raphaël, E. Capillary-Driven Flow Induced by a Stepped Perturbation Atop a Viscous Film. *Phys. Fluids* **2012**, *24* (10), 102111.
(49) Jansen, J. C. Glassy Polymer. In *Encyclopedia of Membranes*; Drioli, E., Giorno, L., Eds.; Springer: Berlin, Heidelberg, 2015; pp 26−60.
(50) Talik, P.; Piotrowska, J.; Hubicka, U. The Influence of Viscosity and Non-Freezing Water Contents Bounded to Different Hydroxypropyl Celluloses (Hpc) and Hydroxypropyl Methylcelluloses (Hpmc) on Stability of Acetylsalicylic Acid. *AAPS PharmSciTech* **2019**, *20* (5), 1−7.
(51) Picker-Freyer, K. M.; Dürig, T. Physical Mechanical and Tablet Formation Properties of Hydroxypropylcellulose: In Pure Form and in Mixtures. *AAPS PharmSciTech* **2007**, *8* (4), 82−90.
(52) Baron Fourier, J. B. J. *Théorie Analytique De La Chaleur*. Chez Firmin Didot, père et fils, 1822.
(53) Cassie, A.; Baxter, S. Wettability of Porous Surfaces. *Trans. Faraday Soc.* **1944**, *40*, 546−551.
(54) Wenzel, R. N. Resistance of Solid Surfaces to Wetting by Water. *Ind. Eng. Chem.* **1936**, *28* (8), 988−994.
(55) Ezazi, M.; Maharjan, A.; Kwon, G. *Self-Healing, Omniphobic Coatings and Related Methods*. US20210261807A1, 2021.

https://doi.org/10.1021/acsmaterialsau.1c00036
ACS Mater. Au 2022, 2, 55−62